Geotextiles and Geomembranes xxx (xxxx) xxx

Contents lists available at ScienceDirect

Geotextiles and Geomembranes

journal homepage: www.elsevier.com/locate/geotexmem

Professional Practice Paper

Case history on failure of a 67 M tall reinforced soil slope

Ryan R. Berg [a,*], James G. Collin [b], Thomas P. Taylor [c], Chester F. Watts [d]

[a] Ryan R Berg & Associates, 2190 Leyland Alcove, Woodbury, MN, 55125-3504, USA
[b] The Collin Group, 7445 Arlington Road, Bethesda, MD, 20184, USA
[c] Ground Improvement Systems, LLC, 114 South Collins Street, Arlington, TX, 76011, USA
[d] Director of Geohazards & Unmanned Systems Research Center, Reed Hall, Box 6939, Radford University, Radford, VA, 24142, USA

ARTICLE INFO

Keywords:
Reinforced soil slope
Geogrid
Failure
Compound failure plane
Case history

ABSTRACT

Construction of this 67 m high *RSS* was completed in December 2006. After seven years in-service, a tension crack was observed at the top of the slope. In March 2015 this *RSS* structure catastrophically collapsed. This *RSS* structure collapsed in a compound failure mode; as the failure plane passed beneath, partially behind, and partially through the reinforced soil mass. The failure plane beneath the *RSS* was along a shale-claystone interface. The failure surface partially behind the *RSS* was along sandstone bedrock with water-seeping bedding planes dipping out of the rock mass. The failure surface through the upper portion of the *RSS* is where the geogrid reinforcement was overwhelmed by stresses originating from underlying deformation. The *RSS* collapse occurred after 8.3 years in-service as the shear strength along the shale-claystone interface decreased and approached the fully softened strength. The primary causative factors of this failure are: (i) an insufficient subsurface investigation program and interpretation of data for design and detailing; (ii) insufficient specifications and construction plan details for both foundation preparation and rock backcut benching; (iii) insufficient foundation preparation and rock backcut benching during construction; and (iv) adaptations to the design made during construction.

1. Introduction

Construction of the tallest reinforced soil slope (*RSS*) in the United States was completed in December 2006, at Yeager Airport, located near Charleston, West Virginia. This 67 m (*m*) high *RSS* structure was designed and constructed as part of the airport's 2005 facility upgrades. The purpose of the *RSS* was to support a 152 *m* extension of Runway 5; on which an engineered mass arresting system for emergency stops was installed. This *RSS* structure catastrophically failed on 12 March 2015; fortunately without loss of life, but it did result in extensive property loss and damage.

This project, the failure of the structure, and this forensic analysis work is unique in several aspects. The *RSS* structure is unique due to its height and the massive amount of geogrid soil reinforcement within it. The structure was in-service for many years and had been performing well. Movements started being observed about two years prior to failure. Therefore something changed, either the resistance decreased or the loading increased, or a combination of the two. The *RSS* suffered a catastrophic collapse, which is infrequent in *RSS* failures. The failure plane passed through approximately 30 *m* of the reinforced soil, and by visual observation, was in internal or compound (Berg et al., 1989) failure mode. Such is rarely seen in *RSS* failures, and certainly none of this magnitude. The failure plane was well defined and therefore could be used in back analyses. Additionally, the structure was convex in plan view, and there were three dimensional (*3D*) aspects to construction, failure, and stability analyses to be considered. To the best of our knowledge, *3D* analysis of a convex, uniaxial geogrid reinforced soil slope had not been attempted prior to this work. Again, *3D* analyses are rarely seen in *RSS* structures and this is the first with a documented failure.

The authors of this case history were members of one of the several engineering teams investigating this failure. Our team worked for the owner's insurance company and then for attorneys representing the owner, Central West Virginia Regional Airport Authority (*CWVRAA*), in litigation. This paper is based upon: (i) our review of design and construction records; (ii) observations during removal of the remaining *RSS* fill and excavation of investigatory trenches; (iii) laboratory testing of soils and geogrids used in construction; (iv) subsequent subsurface investigation (by others) for repair works; and (v) our analyses (Collin et al., 2018). Additionally, some insights were gained from

* Corresponding author.
E-mail addresses: ryanberg@att.net (R.R. Berg), jim@thecollingroup.com (J.G. Collin), tptaylor.pe@gmail.com (T.P. Taylor), cwatts@radford.edu (C.F. Watts).

https://doi.org/10.1016/j.geotexmem.2020.06.003
Received 27 March 2020; Received in revised form 15 June 2020; Accepted 22 June 2020

published/released documents by other investigative teams, though these were limited. Our observations, analyses, discussion, and conclusions documented within may differ from those of other investigative engineering teams.

2. Project background

Initial construction of Yeager Airport near Charleston, West Virginia was completed in 1947, and required excavating several hilltops and filing the adjacent valleys to create a nearly horizontal plateau for the runways and accompanying infrastructure. Because the airport was constructed on hilltop ridges, the ground surface slopes steeply down to the surrounding Elk and Kanawha river valleys on the southern and western perimeters, respectively, of the airport. The length of Runway 5 was extended in 1971.

Runway 5 was extended again in 2005, by an additional 152 *m*. This extension was for a runway airplane engineered material arresting system (*EMAS*), which was required by the Federal Aviation Administration (*FAA*). This extension is supported by the *RSS* structure, construction of which was initiated in September 2005 and completed in December 2006.

The planned *RSS* structure was to be 70 *m* high with a smooth 1:1 slope face that was wrapped with grid and vegetated. The *RSS* structure toes into the natural, approximately 2:1 slope, about 39 *m* above Elk creek. Fill soil for construction of the *RSS* was from onsite airport property borrow sources. The fill material was trucked down from the top of the slope, due to site constraints and operational considerations. Conceptual design, subsurface investigation, final *RSS* design, plans and specifications preparation, and construction observation for this project were completed by a single engineering firm.

3. Subsurface investigations

Subsurface investigations on this project were performed in the following sequence: (i) pre-design, by the project engineer; (ii) during construction, by the contractor and with the project engineer's observation; and (iii) post-failure, as described below. The pre-design phase consisted of several borings. A plan view with boring locations and numbers, and with the outline of the *RSS* shown, is presented in Fig. 1. Pre-design boring logs were located in the project files for most of the proposed borings; however planned borings B-4, B-5, B-10, and B-11 were not drilled. Note that little information was gathered at the base and toe of the proposed *RSS* structure in the borings completed. A summary of these borings focused on rock type and elevation encountered, and groundwater encountered, is presented in Table 1.

A pre-design subsurface investigation report was not located in the project files, and apparently was not prepared. Thus, the design engineers' understanding of the site geology and its impact on both a subsurface investigation program and on design of an *RSS* are not specifically documented.

The interpretation of the subsurface boring program should have identified the following items, each of which should have been addressed prior to finalizing the design and issuing construction drawings. These items include:

(a) There are no borings in the slope beneath the proposed *RSS*. Borings and subsurface information are required in order to check the stability of the slope beneath the *RSS* toe and to confirm the *RSS* is being built upon a firm foundation.
(b) Groundwater was found in three borings, B-2, B-7, and B-12; which were drilled in 2003 on February 26 and 27. This warrants: (i) further investigation as to how the groundwater fluctuates over the course of dry and wet periods; and/or (ii) *RSS* design with chimney drain behind and blanket drain beneath the *RSS* mass. The reinforced slope stability analysis and design must either fully model groundwater flow into and out of the *RSS* or provide drains to keep water out of it.
(c) Shale is clearly identified in several borings, with notation of fissile, ranging in color from light to dark gray to brown, and varying in strength from very soft, to soft, and to medium hard. This material should have been specifically investigated in regard to effect on stability of the *RSS*, construction stripping requirements, and construction benching requirements.
(d) Coal seam(s) are identified in some of the borings. In boring B16, a 0.6 *m* thick layer of soft to very soft brown shale overlies a 0.6 *m* thick layer of coal, that is underlain by 0.6 *m* thick soft to medium

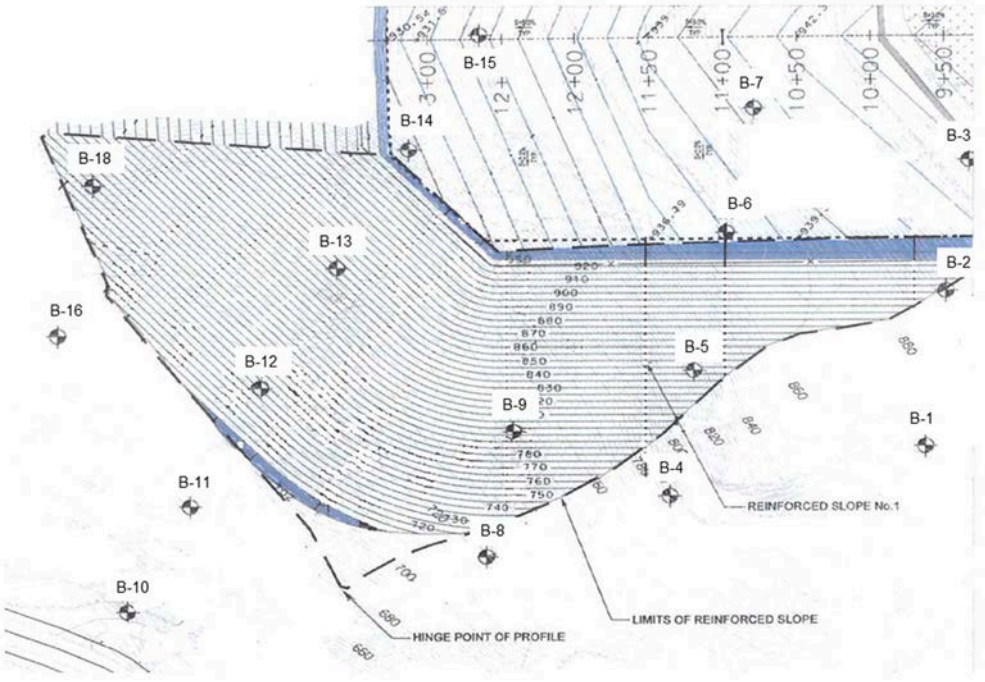

Fig. 1. Proposed RSS plan view with planned boring locations (after Triad Engineering, 2005).

Table 1
Summary of pre-design boring logs at proposed *RSS*.

Boring #	Ground Elevation (ft)	Rock Elevation (ft)	Rock Type and Water Noted
B-1	851	843.5	Sandstone
B-2	902.3	–	Groundwater measured at depth of ~23.3 ft (~EL 879). Boring was noted to be dry immediately following drilling completion. Second sheet of log not included in logs.
B-3	941.5	876.5	Weathered soft to medium hard Sandstone
B-4	–	–	Not drilled.
B-5	–	–	Not drilled.
B-6	858.4	857.2	Poorly cemented and weathered Sandstone
B-7	893.2	NA	FILL. Groundwater measured at ~ EL 877.5.
B-8	718.1	710.6	Gray Shale – fissile, soft
B-9	747.1	741.6	Brown and gray Shale – fissile, soft
B-10	–	–	Not drilled.
B-11	–	–	Not drilled.
B-12	712.3	704.3	Dark gray Shale – fissile, soft to medium hard Groundwater was observed at EL 704.3, top of shale, at time of exploration.
B-13	747.3	736.8	Gray Shale - soft to medium hard
B-14	788.4	788.0	Sandstone hard
B-15	835.5	833.0	Sandstone medium hard
B-16	709.8	704.8	Brown Shale – fissile, soft to very soft, 2 ft thick, underlain by coal, 2 ft thick, underlain by Gray Shale – soft to medium hard
B-17	738.7	736.2	Sandstone
B-18	756.0	748.5	Light gray Shale - soft

Note: 1 ft = 0.305 *m*.

hard gray shale. This formation should have been specifically investigated in regard to its extent, effect on drainage and pore water pressure buildup, stability of the *RSS*, construction stripping requirements, and construction benching requirements.

At the start of construction, the contractor dug several test pits, in conjunction with clearing operations, to determine depth to bedrock. Fulltime construction observation was performed by project engineer personnel. In their daily records, it is noted that "*Test pit excavation was necessary to determine approximate depth and stratification of the underlying bedrock.*" However, no identification or differentiation of rock type was noted in the observation notes, nor in the test pit logs. Additional subsurface information collected during construction was the observation of water seeps, at different times and elevations, along the backcut. In June 2006, the construction observation logs noted "*several seeps along the entire face of the existing Runway 5 end expansion area, which necessitates installation of an under-drain system, immediately. The under-drain system should consist of approximately* 750 LF *of perforated 4" φ SDR 17 High Density Polyethylene Pipe, filter fabric, and drainage stone that meets gradation requirements of #57 limestone.*" The seepage drains were run laterally, at a gentle slope, to discharge on the edge at the *RSS* structure.

Post-failure subsurface investigation included sampling and testing of the (remaining) reinforced soil fill and retained backfill materials; examination and mapping of the exposed rock face (after slide debris removal); geologic evaluation; the excavation of test trenches in the foundation beneath the *RSS* (after slide debris removal); and soil borings by the owner's engineer. Borings were performed to evaluate reconstruction options and for design of the option selected. See Cadden et al. (2019) for details of the reconstruction of Runway 5 safety overrun safety structure.

Density testing, geogrid sample retrieval, and soil sampling was performed during the deconstruction of the reinforced scarp. Density tests, using nuclear density gage, sand cone, and water replacement methods, were used to evaluate the in-place density of the reinforced fill. Nuclear density and sand cone tests were performed in the 150 mm (6 inch) minus processed rock fill just above the geogrid layers and the water replacement test was used in the shot rock (i.e., non-processed) fill above the processed rock fill layers. During the deconstruction 340 nuclear density tests were performed in these two types of fills. The measured dry density, from the nuclear density tests, ranged from 17.1 to 20.2 kN/m^3, with an average of 19.2 kN/m^3 and an average moisture content of 9.4%. Seventy-one (71) sand cone density tests were performed in the processed rock fill lifts. The range of measured dry densities varied from 17.1 to 21.2 kN/m^3 with a moisture range from 6.3 to 12.6%; the averages being 19.1 kN/m^3 and 9.1%. Thirty-two (32) density tests with the water replacement method (ASTM D5030,) were performed in the shot rock fill; and the measured dry densities varied from 17.7 to 22.1 kN/m^3, with a moisture range from 5.3 to 11.4%. The averages were 19.4 kN/m^3 and 8.0%. The weighted average dry density of all three modes of density testing was 19.1 kN/m^3 with a moisture content of 9.3%. The averages from the eight preconstruction Standard Proctor tests, that were used to monitor construction compaction, were 19.5 kN/m^3 density and 11.4% moisture content.

Soil borings through the slide debris and into the underlying rock were performed by seven of the failure investigative parties. A total of 30 borings were drilled. A coal interval was noted on 10 of these borings. The thickness logged varied from 0.1 to 0.5 *m*, and bottom elevation ranged from 208.2 *m* to 209.6 *m* (695.4–700.0 ft). An additional subsurface exploration and a field testing program were performed as part of the design of the replacement structure, a tieback retaining wall (see Cadden et al., 2019). This work included 10 new borings with rock coring and laboratory testing to assess the subsurface conditions below and behind the proposed retaining wall.

Three trenches were exhumed after removal of the *RSS* slide debris to

Fig. 2. Example of shear failure plane identified in the trenches excavated below the base of the RSS. (Photo credit: James G. Collin).

investigate and identify the stratigraphy and the location of the failure surface below the base of the *RSS*. Each trench was orientated in the same direction along a predetermined centerline. The trenches orientation and location were agreed on by the litigants in this case and were in the direction of movement of the *RSS* slide. Sheared failure planes were identified in these trenches and included failure planes of clay over top of coal seam, clay seam on top of rock, and clay to clay interface, see Fig. 2. A sheared failure plane, below a coal seam, on top of hard rock was found in several locations.

Geologically, Yeager Airport and Charleston, West Virginia, lie within the Appalachian Plateau physiographic province. This region consists of flat lying (nearly horizontal) sedimentary rock of Paleozoic age derived from the then tectonically active Appalachian Mountains to the east and deposited within the low-lying continental and shallow-marine environments of the Central Appalachian Basin. Hence, the sedimentary rock sequences, influenced by sea level fluctuations, consist primarily of alternating layers of sandstones, shales, mudstones, and coal seams. Some thin limestone beds are also present.

The shale beds within these formations are also known for the widespread occurrence of swelling clays. These are clays that absorb water and expand when they get wet (personal communication with B. M. Blake). Some of these highly plastic clays were identified as slide surfaces during the post-failure exploratory trenching.

The Charleston East and West topographic quadrangles were mapped in 1976 to identify landslide areas. The quadrangles were remapped, updated and published by the United States Geological Survey (*USGS*) in 1983. The *RSS* structure was placed directly above and on an area shown as active landslide in 1983 (*USGS*).

Mapping the orientations of discontinuities on site is vital to understanding the impacts that structural geology has on performance and overall stability of natural and manmade slopes. Two methods were employed in mapping discontinuities at this site. First, traditional manual mapping was performed, using rope access techniques, on the exposed rock faces. Discontinuity orientations were measured using a standard Brunton transit compass as well as a smart phone application. Secondly, remote mapping was performed using an unmanned aerial system (*UAS*/drone), allowing for the photogrammetric generation of *3D* georeferenced models from which geologic structure data were extracted.

Examination of the stereonets, from both mapping techniques, revealed that the prominent dip directions range from 170 to 230° azimuth, and the dip angles range from about 30 to nearly 90-degrees from vertical. These discontinuity orientations also provide conduits that direct groundwater flow in those same directions from the bedrock directly into the *RSS* and the foundation on which it was placed. Evidence of such flow is obvious in the documented springs and seeps observed on the site, both during construction and deconstruction of the *RSS*.

4. As-designed *RSS* structure

Table 2
Design soil parameters.

Soil Layer	Unit Weight (*kN/m*^{3})	Effective Friction Angle (°)	Cohesion
Reinforced Fill	18.1	36	0
Retained Soil Fill	22.0	40	0
Foundation	22.0	40	0

A reinforced slope design report by the design engineer was not provided in the production of documents. However, computer generated output for several *RSS* sections from the ReSSA software (ADAMA Engineering, Inc, 2001) were provided. It appears that preliminary designs were performed in 2003 and additional designs were performed in 2004.

Table 3
As-designed and specified *HDPE* geogrid tensile strength properties, and as-designed geogrid-soil interaction properties.

Geogrid Grade	Tensile Strength Properties					Interaction Properties		
	T_{ult} (*kN/m*)	RF_{ID}	RF_D	RF_{CR}	T_{al} (*kN/m*)	C_{ds}	C_i	α
P1	193	1.2	1.1	2.60	56.3	0.8	0.8	0.8
P2	186	1.2	1.1	2.60	54.3	0.8	0.8	0.8
P3	149	1.2	1.1	2.60	43.3	0.8	0.8	0.8

Based on a review of these computer runs it appears that the target design factor of safety (*FS*) for the *RSS* was 1.30, and two-dimensional (*2D*) limit equilibrium analyses were used to determine the factors of safety. Fully drained conditions were assumed. The soil and geogrid properties utilized in the 2004 design are provided in Tables 2 and 3, respectively.

The *RSS* design presented on the construction drawings showed full length reinforcements across the full height of the structure. At the planned 70 *m* maximum height of the *RSS*,[1] the reinforcement lengths were 53.4 *m* long across the full height and in the central 75 *m* width of the structure. However, the pre-design borings clearly showed that bedrock would be encountered and a significant amount of soil reinforcement was shown to be installed in bedrock.

Neither the construction drawing notes nor the construction specifications addressed placement of geogrid in the zone of bedrock. No detailed documentation between the design engineer and contractor, and/or with the owner, on this issue was discovered in our investigation. Likewise, neither rock excavation nor rock backcut benching were addressed in the construction drawing notes or specifications. The stripping specification simply stated *"In areas designated to be cleared and grubbed, all stumps, roots, buried logs, brush, grass, and other unsatisfactory materials shall be removed, . ."* and did not address stripping of soil to rock; nor does it define competent rock.

The reinforced soil fill was specified to consist of durable sandstone from onsite excavations. This fill had a wide acceptable gradation; with an allowable percentage of 0–50 percent passing the No. 200 sieve. Thus, the *RSS* mass could be constructed with a material ranging from high to very low permeability. Neither a chimney nor blanket drain were called for in the construction drawings or specifications.

The design engineer's analysis model for the maximum height section, as shown on the construction drawings, is shown in Fig. 3. Depth to rock was shallow and a little below the existing ground line shown and thus, either rock had to be removed to install the geogrid or the geogrids lengths would have to be shortened. However, neither option was noted. A front elevation view, as shown on the construction drawings, is presented in Fig. 4. The zones of where the three different grades of geogrids and the geogrid lengths are noted. The V-notch is the hinge point of this convex shaped (in plan view) *RSS* structure.

5. As-built *RSS* structure

The as-built *RSS* structure varied significantly from the as-designed, detailed, and specified structure. Two grades of polyester (*PET*) geogrids (see Table 4) were used in lieu of the three grades of high density polyethylene (*HDPE*) geogrids (see Table 3). *PET* grade 1 was used for *HDPE* grades 1 and 2; and *PET* grade 2 was used in lieu of *HDPE* grade 3. This change resulted in one grade of geogrid being used across the full height of the structure along the central, maximum height portion of the structure.

The reinforced soil fill was generally granular, and most often

[1] There was a discrepancy between drawings on the planned *RSS* height. There are also some small discrepancies on the final constructed height, due to various records and field changes.

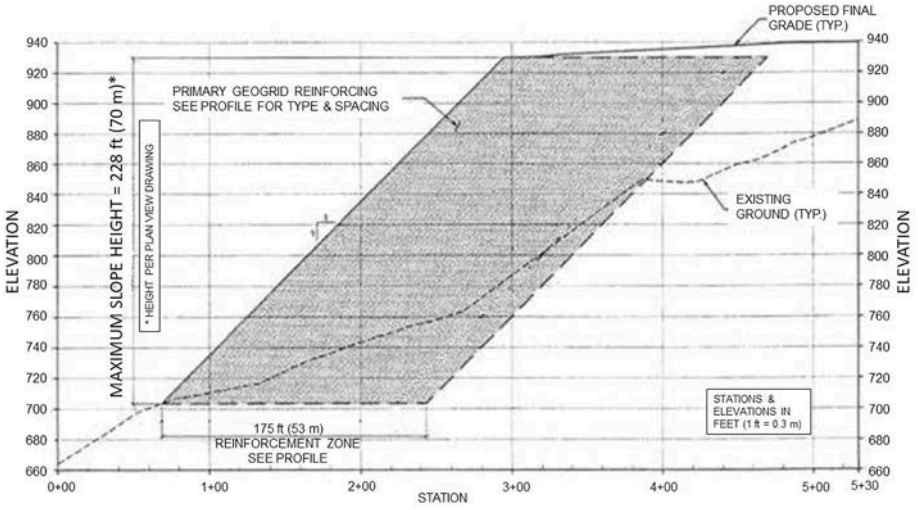

Fig. 3. Construction plan cross section, at maximum height (after Triad Engineering, 2005).

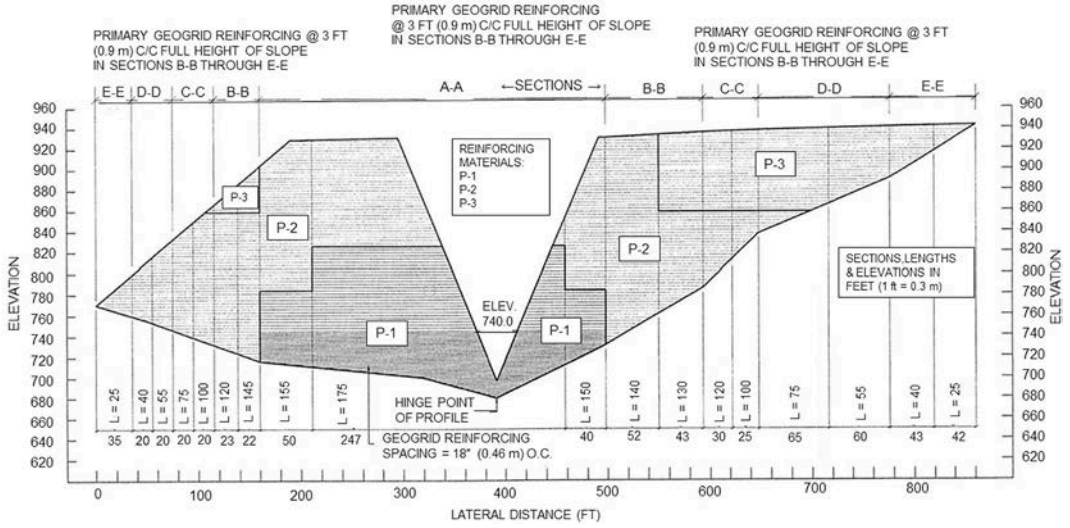

Fig. 4. Construction plan front elevation view of RSS (after Triad Engineering, 2005).

Table 4
As-built *PET* geogrid tensile strength properties.

Geogrid	T_{ult} Case	T_{ult} (kN/m)	RF_{ID}	RF_D	RF_{CR}	T_{al} (kN/m)
P1 and P2	Specified	187.8	1.30	1.15	1.90	66.1
P3	Specified	145.2	1.34	1.15	1.90	49.6
P1 and P2	Measured[1]	146	n/a[2]	1.0[3]	1.72[4]	84.8

1. Average strength of samples tested from geogrid recovered from the intact area behind the scarp, as measured in single rib testing (ASTM D6637).
2. Ultimate strength of exhumed samples is inclusive of installation damage and, therefore, RF_{ID} is not applicable in computation of the T_{al} value.
3. Value assumed for 8.3 years in-service.
4. Reduction factor value listed by the geogrid manufacturer on project submittal.

labelled as crushed stone in field observation notes. This material is much more granular than the specification allowance of up to 50% fines. Though not a free-draining material, this fill should be *relatively* free-draining as compared to the in situ retained backfill soils. However, clays and silts were noted in some of the reinforced fill compaction test descriptions and thus, some compacted soil layers (or zones within a layer) may be significantly less permeable than adjacent layers.

The bottom of the reinforced fill started at elevation 216.4 *m* (710 ft), which is 3 *m* above the planned elevation. This revision was at the contractor's request and due to constructability issues of placing fill and geogrids in the V-notch (see Fig. 4) detailed at the *RSS* toe. This lower 3 *m* was constructed with a rock fill to create a working platform, wide enough to start installation of reinforced fill and geogrids.

The as-built reinforcement lengths, in the lower 2/3 height and in the central 75 *m* width of the *RSS*, were modified from the design length of 53.4 *m* to lengths that varied from 22 *m* to 53.4 *m,* extending back to the rock face, or close to the rock face. The geogrid lengths at each lift were detailed in the construction observation notes. Comparison of the documented lengths to exposed backslope rock face (after post failure debris removal) indicated that the geogrids did not always extend to the rock face. In some cases, this appeared due to maintenance of the haul road for bringing on-site fill from the northwest quadrant of the airport property down the backslope to the fill area. In other cases where the geogrid did not extend to the rock face, it was interpreted as incomplete stripping of soil.

6. Performance and failure

Construction of the *RSS* structure commenced on 28 September

2005. The construction of the *RSS* structure was completed in December 2006. This was followed by construction of the runway pavement extension and installation of the *EMAS*. Soil sloughing at the toe of the *RSS* was first observed approximately 4 years after the completion of construction. This was attributed to soil erosion at the toe of the *RSS* structure and deemed a surficial slope failure by the design engineer. These surficial failures occurred several times over the next 4 years. The constructed reinforced slope started to show movement above the crest of the slope in 2013, after seven years in-service. By February 2014, large deformations and tension cracks were visible in the slope crest, in the *EMAS* portion of the runway, as shown in Fig. 5. Investigators re-examined the *RSS* toe and did not attribute crest cracking to any new sloughing or erosion.

The slope catastrophically failed (see Fig. 6) on 12 March 2015 after 8.3 years in-service. The failure plane propagated through the reinforced soil mass, resulting in a head scarp that was near vertical for approximately 30 *m* in height (see Fig. 7). The failure surface sheared through more than 30 layers of geogrid, each layer had a manufacturer published minimum average roll value, *MARV* (ASTM D4439,), ultimate strength of 187.8 kN/m, throughout the exposed head scarp. Rupture of the soil reinforcement in a failed *RSS* seldom occurs, and never to the magnitude observed at the Yeager failure.

This *RSS* structure was in-service and performing adequately after it was constructed. Then, after 7 years in-service, a tension crack on top of the *RSS* was observed at a distance back from the crest of 53 *m* (the length of the geogrid layers), and monitoring of it began. Then about one month prior to collapse, a 0.8 *m* scarp developed over the reinforced soil mass at an approximate distance back from the slope crest of 28 *m*, as shown in Fig. 5. Something was changing with this structure, either the stability resistance was decreasing or the loading was increasing, or a combination of the two. On 12 March 2015, with 8.3 years in-service, this 67 *m* high *RSS* structure suffered a catastrophic collapse, as shown in Figs. 6 and 7.

7. Stability analyses summary

Three stability analysis methods were used to investigate the failure of this *RSS* structure. The analysis started with *2D* limit equilibrium analyses to investigate the observed failure, and could vary resistances and loadings to examine effect on *FS* values and failure plane locations. Analyses were refined after excavation of the failed material, the foundation investigation trenches, and laboratory testing of the soils and geogrid soil reinforcements. Resistance was parametrically decreased along the foundation shale-claystone interface. Loading in the stability analyses was increased with a range of four groundwater levels to investigate and quantify the effect on stability of the *RSS* structure. Groundwater measurements within the in-service *RSS* were not measured. Therefore, likely ranges of groundwater conditions were estimated for use in stability failure analyses. To estimate the maximum likely groundwater potentiometric surface two-dimensionally, potential piezometric groundwater levels and destabilizing water pressure values, based on principles of hydraulic head under semi-confined conditions, were used. It was assumed that the zone between the fill and the native rock (boundary transition area) becomes saturated first with water from bedrock seeps and/or infiltrating surface water. Water pressure started at zero at the upper end of the saturated boundary. It was then assumed to build to a maximum pressure halfway through the profile vertically; and then, pressure tapered off to zero at the toe of the slope. This model Models I and II from Hoek and Bray (1981). Four different groundwater tables of none (dry), low, medium and high were used to parametrically investigate effect of groundwater on the stability of the *RSS*.

Finite difference numerical modeling analyses (*2D*) were used to model construction sequences and to further the understanding of the failure kinematics. These analyses successfully matched the observed crest deformation and collapse failure plane within the reinforced mass, the crest tension crack observed behind the reinforced mass the year before collapse, and the geogrid rupture and *RSS* collapse. The analyses

Fig. 5. Deformation at top of RSS structure and within the reinforced soil zone, approximately 1 month prior to collapse. (Photo credit: *CWVRAA*).

Fig. 6. Aerial failure photo, prior to debris mass creeping over and destroying the church. (Photo credit: W.VA. National Guard).

Fig. 7. Photo of 30 *m* high failure scarp through the reinforced mass. (Photo credit: Ryan R. Berg).

Table 5
Summary of *2D* and *3D* limit equilibrium stability analyses.

Case - Description	Geogrid Strength	Foundation Strength	Ground-water	*2D FS*	*3D FS*
Analysis of As-Constructed and Specified	$T_{al\text{-}specified}$ = 66.1 kN/m	As Assumed	Dry	1.45	1.44
End of Construction – foundation soil at peak strength	$T_{ult\text{-}measured}$ = 146 kN/m	Peak	Dry	1.70	1.75
End of Construction – foundation soil at fully softened shear strength	$T_{ult\text{-}measured}$ = 146 kN/m	*FSS*	Dry	1.15	1.27
			Low	1.15	1.26
			Medium	1.13	1.21
			High	1.13	1.13
Failure – geogrid strength reduced for creep; foundation soil at fully softened shear strength	$T_{ult\text{-}measured}/RF_{CR}$ = 84.8 kN/m	*FSS*	Dry	1.03	1.08
			Low	1.01	1.07
			Medium	0.99	1.03
			High	0.95	0.95

used a strength reduction factor for the foundation shale-claystone interface to investigate movements (strains), loads (stress), and collapse mechanism.

Additionally, *3D* limit equilibrium analyses were performed to investigate the effect of the *RSS* convex shape on stability. This used the observed failure geometry and a foundation shear extrapolated from the investigation trenches. Samples retrieved from the trench exploration were tested to determine their fully softened and residual strengths for foundation shale-claystone interface.

Details of the stability analyses are presented in Collin et al. (2020); where the reinforced soil fill, retained soil backfill, reinforced fill rock backslope interface, foundation clay seam, and geogrid strength properties are summarized. Additionally, the soil fill unit weights and the four assumed phreatic surfaces are presented. There are three different geogrid strengths discussed and used within these analyses. This includes the long-term strength, T_{al}; that is computed as the quotient of the ultimate tensile strength, T_{ult}, over the product of reductions factors for creep, RF_{CR}, installation damage, RF_{ID}, and degradation, RF_D. The specified ultimate tensile strength is the *MARV* of the geogrid determined from a rapid tensile test (ASTM D6637,); by the manufacturer. Specified T_{al} values are presented in Tables 4 and 5.

In addition to $T_{al\text{-}specified}$, the $T_{ult\text{-}measured}$ and $T_{ult\text{-}measured}/RF_{CR}$ strengths were used for the P1 geogrids in the stability analyses. The measured ultimate strength was based upon samples tested from geogrid recovered from the intact area behind the scarp, as measured in single rib testing (ASTM D6637,). Single rib testing was used in lieu of multi-rib testing, where strength measurements may be skewed low when zipping type failures occur due to heavier installation damage on a particular rib and laboratory techniques. Ultimate strength of exhumed samples is inclusive of installation damage and, therefore, RF_{ID} is not applicable in computation of the $T_{ult\text{-}measured}$ value. The $T_{ult\text{-}measured}$ strength was used for the end-of-construction analyses when degradation would not have occurred, and it was assumed that creep time was insignificant. The analysis of as-constructed and failure cases used the $T_{ult\text{-}measured}$ strength reduced by the creep reduction factor, RF_{CR}. A creep reduction value of 1.72, as listed by the geogrid manufacturer on their project submittal, was used.

The geogrid anisotropic strength relationship was required for the *3D* limit equilibrium analyses. The ultimate strength of the geogrid across the 90° angle, from the machine (i.e., roll) direction to the cross machine direction, was required as the slope failure plane spanned this range. An initial testing program was performed using virgin samples of the P1 type and grade of geogrid. Samples were cut from a roll at angles of 0, 22.5, 45, 67.5, and 90° from roll direction. Wide width rapid tensile tests (ASTM D4595,) were performed with the samples clamped in the roll direction. There was some slippage of individual ribs in the 22.5, 45, 67.5, rotated cut samples and, therefore, some engineering interpretation was used with those test results. This testing and interpretation led to anisotropic geogrid strength definition, as rotated 90° from machine direction to cross machine direction, that decreased linearly from 100% T_{ult} at 0° to 10% T_{ult} at a 60° rotation, and then was constant at 10% T_{ult} from a rotation of 60–90°. Initial *3D* analyses demonstrated that the computed *FS* values were not significantly affected by this anisotropic strength definition. Thus, additional testing and refinement of the relationship was deemed unwarranted.

The geology and soils information gained from the combination of the subsurface investigations (previously discussed), as illustrated in Fig. 8, was used for the stability analyses. A cross section for the *2D* failure analysis for the dry water assumption, with critical failure plane, is presented in Fig. 9. The stress pattern and failure surface from the numerical modeling is shown in Fig. 10. In all cases analyzed, the emergence of the shear failure surface is close (3 *m*) to the one observed in the field, 28 *m* back from the slope crest. The numerical analyses also found of a high stress zone at 53 *m* behind the crest where, after 7 years in-service, a tension crack on top of the *RSS* was observed. Results of the stability analyses are presented and discussed in Collin et al. (2020), and are summarized in Table 5.

8. Discussion

The initial design was deficient in its use of a minimum acceptable stability *FS* value of 1.3. This value is at the low end of acceptable stability *FS* and may be used for typical type and height *RSS* structures, where geotechnical parameters are well defined, and where the *RSS* is non-critical. The Yeager Airport *RSS* was an atypical height structure, and far exceeded previously constructed structures. Though a geotechnical investigation was performed as part of the design process, it was insufficient as it did not thoroughly investigate and define the *RSS* foundation conditions. This was a critical *RSS* structure. As now clearly documented, post-failure and after replacement structure construction, the cost of failure far exceeded the initial construction costs. Furthermore, there was a potential for loss of life with failure of this *RSS* structure, as evidenced by the church and homes below the slope that were destroyed by the failure debris. As such, this structure certainly should have been deemed critical.

If the geotechnical parameters had been well defined, a minimum acceptable stability *FS* of at least 1.5 (Berg et al., 2009) to 2.0 (Duncan and Wright, 2005) should have been used for design of this *RSS* structure. A *FS* value greater than 1.5 should have been contemplated with consideration of the height and criticality this structure, the *3D* stability aspects and limitations of available analysis tools, and with the inadequacies of the subsurface investigation.

The as-constructed stability *FS* was below the 1.3 design value, due to several factors. The inadequate subsurface investigation resulted in an unconservative foundation design strength. The failure to remove the seams of weak foundation soils and to bench the rock backcut resulted in higher stresses along these interfaces, and resulted in a preferred failure plane beneath, behind, and through the *RSS* structure.

The original design and revised design were based on the assumption that the *RSS* was drained. Although the reinforced fill was granular, the lack of a chimney drain behind and a blanket drain beneath the *RSS* could result in groundwater infiltrating from the fractured sandstone

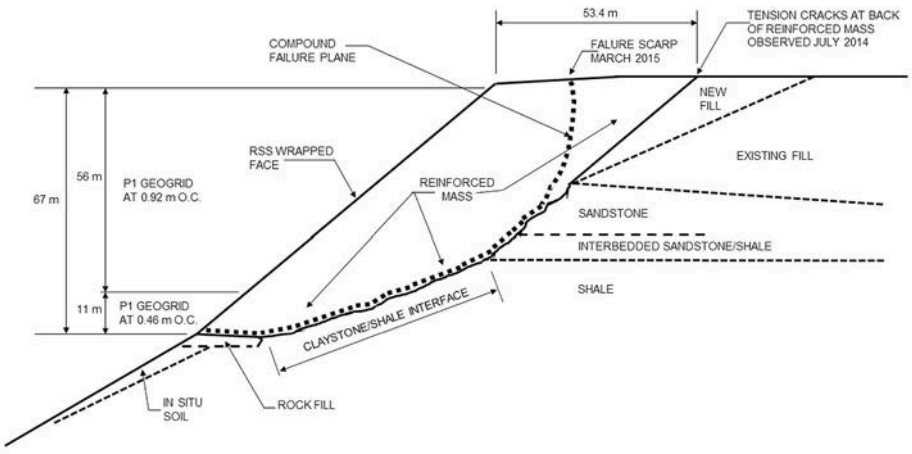

Fig. 8. Cross-section of RSS with failure surface and soil/rock stratigraphy shown.

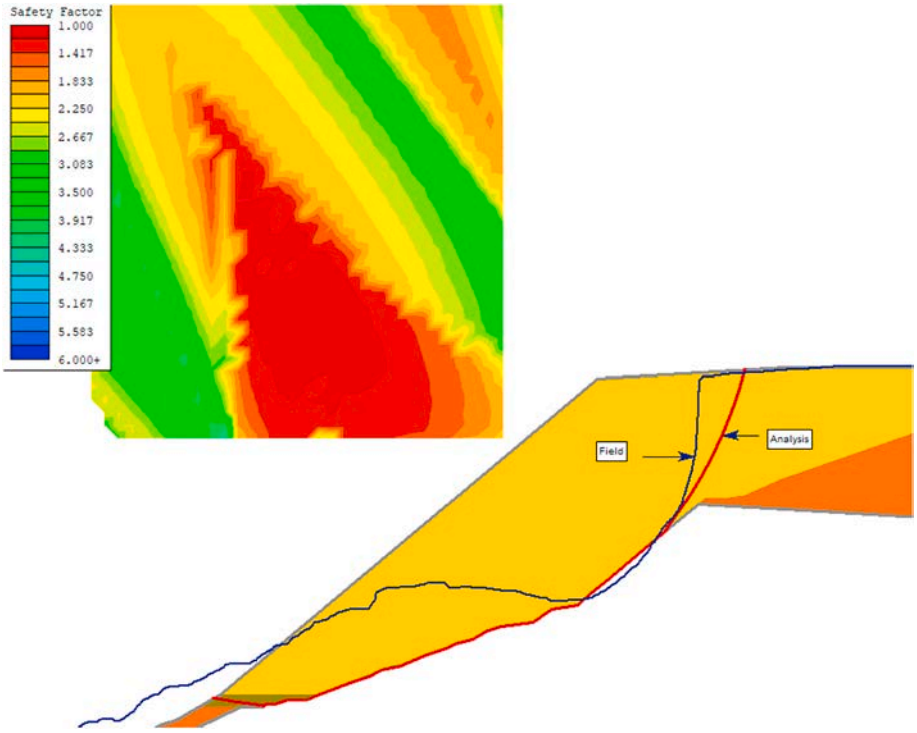

Fig. 9. *2D* limit equilibrium analyses cross section and critical failure plane, with post-collapse geometry with debris surface, and field observed and analysis predicted scarps noted.

into the *RSS*. For the end of construction and failure conditions, four different groundwater tables (none (dry), low, medium and high) were considered in the stability and deformation analyses. Such may have been seasonal variations. The variable groundwater levels that were considered, appear to have limited impact on the computed stability *FS*. However, long-term fluctuating seepage into the *RSS* from bedrock structures, including rock joints and open bedding planes, as identified on-site, is known to weaken susceptible materials over time. This happens through water-driven chemical weathering, leading to softening and decreased strength, as well as from material fatigue caused by alternating high and low pore water pressures.

This *RSS* structure was initially stable for seven years, and then progressively failed over the next two years. The failure plane, along the center of the failed mass, passed beneath, then behind, and then through the upper portions of the *RSS* structure, (i.e., compound failure plane mode). Movements (strain) occurred along this failure plane. In the foundation, the forensic trench documented the failure plane was located in the clay soil/rock interface, adjacent to a persistent coal seam. Material retrieved from the forensic foundation trench was tested, using a modified Bromhead ring shear apparatus (Stark and Eid, 1998). Testing found fully softened shear (*FSS*) strengths ranging from 25.8° to 19.7°, and residual shear strengths ranging from 20.2° to 14.3°, for normal stresses ranging from 50 to 400 kN/m^2. Limit equilibrium and deformation analyses showed the *RSS* failure occurred at a shear strength approaching, but not at, fully softened.

Behind the *RSS* mass, the failure plane followed the face of the relatively smooth and inclined sandstone rock (see Fig. 11). This rock face was fully exposed with slide debris removal. Movements along this interface may have mobilized residual interface shear strength. However, interface shear strength testing was not performed to quantify interface properties as our investigation deemed the foundation clay layer to be critical.

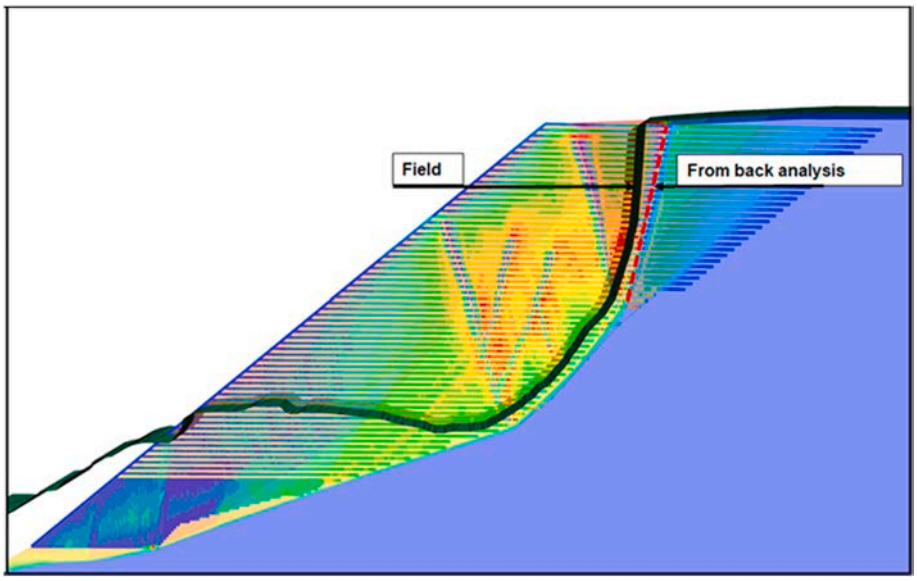

Fig. 10. Numerical modeling cross section with stress pattern at collapse (with stress levels increasing from blue to red) and post-collapse geometry with debris surface, and with field observed and back-analysis predicted scarps noted.

Fig. 11. Relatively smooth (non-benched) rock slope behind the RSS structure, after removal of slide debris. (Photo credit: Ryan R. Berg).

This compound failure plane then passed approximately vertical through about 30 layers of high strength, uniaxial geogrids. There is strain-compatibility between the reinforced fill and the embedded geogrid. The tension crack above the slope crest in 2013 progressed to large deformations by February 2014, prior to the March 2015 collapse. These movements indicate a mobilization of reinforced fill strength and, thus, a mobilization of strain, and therefore stress, in the geogrids. The geogrid strains increased under the larger deformations to a point where creep rupture was imminent. The geogrid layers ruptured and the *RSS* structure catastrophically collapsed on 12 March 2015.

The failure mechanism and primary contributors to failure are discussed above. Additional contributors to the failure are listed in Table 6, with a brief summary of why our investigative team deemed these as contributors.

A comprehensively designed *RSS* would have been designed for minimum stability *FS* of 1.5, or higher. To achieve this, the primary features modified from the original design would include the following: The *RSS* base is founded on competent rock, by identification and removal of weak interface seams. The backcut into the rock is benched to distribute overburden fill stresses, and to lock the *RSS* into the rock backcut, thus raising the compound and global stability factors of safety above 1.5. A chimney drain along the backcut and a blanket drain beneath the *RSS* are included to discharge any subsurface water entering the *RSS*. The number and/or strength of geogrid layers are increased to take the internal stability *FS* from 1.3 to 1.5, or higher. Additionally, the *RSS* face is benched, to reduce water runoff flow velocities and erosion, and includes intermediate wide benches for maintenance, safety, and monitoring purposes.

9. Conclusions

The Yeager Airport *RSS* structure and its failure was unique in several aspects. The *RSS* structure was exceptional due to its 67 *m* height and the massive amount of high strength uniaxial geogrid soil reinforcement within it; the structure was in-service for approximately 7 years when cracking was first observed in the runway it supported; and this *RSS* structure catastrophically collapsed after 8.3 years in-service, in a compound failure mode.

The failure of this *RSS* is a result of many contributing factors and deficiencies. Primary contributing factors are: (i) an insufficient subsurface exploration program and interpretation of data for design and detailing; (ii) insufficient specifications and construction plan details for both foundation preparation and rock backcut benching; and (iii) insufficient foundation preparation and rock backcut benching during construction; and (iv) adaptations of the design made during construction of the *RSS* by the contractor and/or design engineer. The weak shale-claystone interface layers below the base of the *RSS,* that underwent strength reduction over time, were not identified in the subsurface investigation, nor were they considered in design or removed during construction. The weak rock-soil interface layers and the failure to bench the rock-face backcut significantly reduced the *FS* of the *RSS* to a critical level and resulted in a compound failure mode collapse.

This critically low *FS* of the slope decreased as the weak cohesive foundation soil layer shear strength decreased; and as movements occurred post-peak shear strengths in the reinforced fill and the reinforced fill-sandstone rock interface may have been mobilized. The lack of internal drainage contributed to the reduction of shear strength within the weak cohesive foundation soil layer; and likely resulted in additional destabilizing forces. However, the stability analyses with watertable variations show the effect on computed safety factors to be

Table 6
Additional contributors to *RSS* failure.

Contributor	Discussion
Inadequate subsurface and geologic investigation	Led to not identifying and addressing weak rock/soil interface associated with shale-claystone interface; to founding the toe of *RSS* on a mixture of soil and rock surfaces, and above previous landslide area; and to an incomplete understanding of potential subsurface water impact. The subsurface investigation performed and the *RSS* design indicate that the site geology was not well understood and/or was not adequately considered in design.
Poor or incomplete design detailing on construction drawings and construction specifications	Construction drawings showed 53.4 *m* long geogrid layers even though the subsurface investigation clearly defined rock within that distance, in the lower ~2/3 of the *RSS*. This led to field modification of geogrid lengths, with little to no construction drawing or specification guidance. Benching of the back rock face was not detailed or specified. Drainage behind and beneath the *RSS* was not detailed or specified. Stripping foundation and backcut to competent rock, and benching the rock backcut were not addressed in the plans or specifications; resulting in the critical compound failure plane in the as constructed *RSS* structure.
No chimney drain	Water infiltrating into the compacted granular reinforced soil fill could have caused some hydroconsolidation. This in turn, would have created additional strains and stress within the reinforced mass and along the backcut sandstone rock interface, particularly along the preferred failure plane.
No blanket drain	Water infiltrating the RSS mass and reaching the foundation would aid the strain softening of the shale-claystone interface; again, along the preferred failure plane.
Lack of peer review	A structure that significantly exceeds the magnitude of established design and construction heights should be peer reviewed. A strong theoretical basis of design and material properties is vital when extrapolating beyond known and proven limits.
Constructability	Reinforcement placement "V" shape at the base of the RSS at the maximum height section as shown on the construction plans, see Fig. 4, was not practical or constructible. A minimum base width is needed to operate equipment, and to install fill and soil reinforcement. The lower 3 *m* of the RSS structure was constructed as an unreinforced rock fill, to create a working bench to start fill and reinforcement placement. Fill, being hauled from the top down, required a haul road to be maintained. In some areas, this prevented installation of reinforcement to bedrock.
Lack of monitoring program	A monitoring program including inclinometers, piezometers, and strain gages on the geogrid would have provided critical information on the performance of the *RSS* prior to collapse and could have led to remediation prior to collapse.
Incomplete evaluation of observed tension crack	The construction records contained detailed documentation of the geogrid lengths at each elevation. Had this been studied and plotted on a cross section after the tension cracks were observed (~2 years prior to collapse) a useful picture of the likely movement/failure plane would have emerged; and could have led to remediation prior to collapse.

minor.

The large crest deformation of approximately 0.8 *m* that formed within the reinforced mass (see Fig. 5) approximately one month prior to collapse along this plane was a sign of impending failure of the *RSS*. Significant movement within the reinforced soil mass resulted in additional strain in both the soil and the geogrid soil reinforcement. As the soil exceeded its peak strength, additional load was shed to the geogrid soil reinforcement. The increased load on the geogrid mobilized creep of the geogrid that, in-turn, created more movement and load shedding to the geogrid; eventually leading to geogrid failure. Such failure would likely be progressive, though relatively quick, as zones of geogrid within the reinforced mass fail and result in higher loads on remaining layers of geogrid.

Declaration of competing interest

The authors declare that they have no known competing financial interests or personal relationships that could have appeared to influence the work reported in this paper.

Acknowledgments

The authors would like to gratefully acknowledge support from the *CWVRAA* and the *CWVRAA*'s insurance company, and their attorneys. The authors would also like to acknowledge documented work of other engineering investigation teams; specifically, the expert report prepared by Exponent.

References

STM D4439. Standard Terminology for Geosynthetics, ASTM International, West Conshohocken, PA, USA.

STM D4595. Standard Test Method for Tensile Properties of Geotextiles by the Wide-Width Strip Method, ASTM International, West Conshohocken, PA, USA.

STM D5030. Standard Test Methods for Density of Soil and Rock in Place by Water Replacement Method in a Test Pit, ASTM International, West Conshohocken, PA, USA.

STM D6637. Standard Test Method for Determining Tensile Properties of Geogrids by the Single or Multi-Rib Tensile Method, ASTM International, West Conshohocken, PA, USA.

ADAMA Engineering, Inc, 2001. ReSSA: Reinforced Slope Stability Analysis, developed under contract with Federal Highway Administration. Newark, DE.

Berg, R.R., Chouery-Curtis, V.E., Watson, C.H., 1989. Critical failure planes in analysis of reinforced slopes. In: Proceedings of Geosynthetics '89 Conference, San Diego, CA, pp. 269–278.

Berg, R.R., Christopher, B.R., Samtani, N.C., 2009. Design and Construction of Mechanically Stabilized Earth Walls and Reinforced Soil Slopes, FHWA NHI-10-024 Vol I and NHI-10-025 Vol II. U.S. DOT, Federal Highway Administration, Washington, D.C., 306p. (Vol I) and 378p. (Vol II).

Cadden, A., Brill, G., Senior, M., 2019. Yeager Airport: Deconstruction and Reconstruction of the Side of a Mountain. Proceedings of Geosynthetics Conference, Houston, TX, pp. 713–719.

Collin, J.G., Watts, C.F., Berg, R.R., Taylor, T.P., 2018. Yeager Airport Reinforced Soil Slope Failure Analysis. The Collin Group, Ltd, (Privileged and Confidential, Prepared at the Request of Counsel).

Collin, J.G., Stark, T.D., Lucarelli, A., Taylor, T.P., Berg, R.R., 2020. Yeager airport reinforced soil slope: 2D/3D stability and deformation analyses. Journal of Geotechnical and Geoenvironmental Engineering, ASCE, submitted for publication. Submitted for publication.

Duncan, J.M., Wright, S.G., 2005. Soil Strength and Slope Stability. John Wiley & Sons, Hoboken, NJ, p. 297p.

Hoek, E., Bray, J., 1981. Rock Slope Engineering, revised Third Edition,. Taylor & Francis Group, London and New York.

Stark, T.D., Eid, H.T., 1998. Performance of three-dimensional slope stability methods in practice. *Journal of Geotechnical and Geoenvironmental Engineering*, ASCE 124 (11), 1049–1060. November.

Triad Engineering Inc, 2005. *Runway 5, Runway 23, and Taxiway "A" Safety Area Improvements*, Construction Drawings Prepared for Central West Virginia Regional Airport Authority, FAA A.I.P. Project No. 3-54-0003-031-2003, Yeager Airport, Charleston, WV, 71 Sheets.

USGS, 1983. Open-File Report OF-83-80: Landslides and Related Features, West Virginia and Ohio; Charleston 1 Degree by 2 Degrees Sheet.